



Contents lists available at ScienceDirect

# Journal of Rock Mechanics and Geotechnical Engineering

journal homepage: [www.rockgeotech.org](http://www.rockgeotech.org)

## Full Length Article

# Application of artificial neural networks for predicting the impact of rolling dynamic compaction using dynamic cone penetrometer test results



R.A.T.M. Ranasinghe\*, M.B. Jaksa, Y.L. Kuo, F. Pooya Nejad

School of Civil, Environmental and Mining Engineering, University of Adelaide, Adelaide, Australia

## ARTICLE INFO

### Article history:

Received 12 August 2016

Received in revised form

22 October 2016

Accepted 9 November 2016

Available online 27 February 2017

### Keywords:

Rolling dynamic compaction (RDC)

Ground improvement

Artificial neural network (ANN)

Dynamic cone penetration (DCP) test

## ABSTRACT

Rolling dynamic compaction (RDC), which involves the towing of a noncircular module, is now widespread and accepted among many other soil compaction methods. However, to date, there is no accurate method for reliable prediction of the densification of soil and the extent of ground improvement by means of RDC. This study presents the application of artificial neural networks (ANNs) for a priori prediction of the effectiveness of RDC. The models are trained with in situ dynamic cone penetration (DCP) test data obtained from previous civil projects associated with the 4-sided impact roller. The predictions from the ANN models are in good agreement with the measured field data, as indicated by the model correlation coefficient of approximately 0.8. It is concluded that the ANN models developed in this study can be successfully employed to provide more accurate prediction of the performance of the RDC on a range of soil types.

© 2017 Institute of Rock and Soil Mechanics, Chinese Academy of Sciences. Production and hosting by Elsevier B.V. This is an open access article under the CC BY-NC-ND license (<http://creativecommons.org/licenses/by-nc-nd/4.0/>).

## 1. Introduction

Soil compaction is one of the major activities in geotechnical engineering applications. Among many other soil compaction methods, rolling dynamic compaction (RDC) is now becoming more widespread and accepted internationally. The RDC technology emerged with the first full-sized impact roller from South Africa for the purpose of improving sites underlain by collapsible sands in 1955 (Avalle, 2004). Over the years, the RDC concept has been refined with updated and improved mechanisms. Since the mid-1980s, impact rollers have been commercially available and are now adopted internationally using module designs incorporating 3, 4 and 5 sides.

The 4-sided impact roller module consists of a steel shell filled with concrete to produce a heavy, solid mass (6–12 tonnes), which is towed within its frame by a 4-wheeled tractor (Fig. 1). When the impact roller traverses the ground, the module rotates eccentrically about its corners and derives its energy from three sources: (1) potential energy from the static self-weight of the module; (2)

additional potential energy from being lifted about its corners; and (3) kinetic energy developed from being drawn along the ground at a speed of 9–12 km/h. As a result, the impact roller is capable of imparting a greater amount of compactive effort to the soil, which often leads to a deeper influence depth, i.e. in excess of 3 m below the ground surface in some soils (Avalle, 2006; Jaksa et al., 2012), which is much deeper than 0.3–0.5 m generally achieved using traditional vibratory and static rollers (Clegg and Berrangé, 1971; Clifford, 1976, 1978). Furthermore, it is able to compact thicker lifts, in excess of 500 mm, which is considerably greater than the usual layer thicknesses of 200–500 mm (Avalle, 2006) and can also operate with larger particle sizes.

Moreover, RDC is more efficient since the module traverses the ground at a higher speed, about 9–12 km/h, compared with traditional vibratory rollers which operate at around 4 km/h (Pinard, 1999). This creates approximately two module impacts over the ground each second (Avalle, 2004). Thus, the faster operating speed and deeper compactive effort make this method very effective for bulk earthworks. In addition, it also appears that prudent use of RDC can provide significant cost savings in the civil construction sector. Due to these inherent characteristics of RDC, modern ground improvement specifications often replace or provide an alternative to traditional compaction equipment. It has been demonstrated to be successful in many applications

\* Corresponding author.

E-mail address: [tharanga.ranasinghe@adelaide.edu.au](mailto:tharanga.ranasinghe@adelaide.edu.au) (R.A.T.M. Ranasinghe).

Peer review under responsibility of Institute of Rock and Soil Mechanics, Chinese Academy of Sciences.



Fig. 1. The 4-sided impact roller and tractor.

worldwide, particularly in civil and mining projects, pavement rehabilitation and in the agricultural sector (Avalle, 2004, 2006; Jaksa et al., 2012).

To date, a significant amount of data has been gathered from RDC projects through an extensive number of field and case studies in a variety of ground conditions. However, these data have yet to be examined holistically and there currently exists no method, theoretical or empirical, for determining the improvement in in situ density of the ground at depth as a result of RDC using dynamic cone penetrometer (DCP) test data. The complex nature of the operation of the 4-sided impact roller, as well as the consequent behavior of the ground, has meant that the development of an accurate theoretical model remains elusive. However, recent work by the authors in relation to RDC, as well as by others in the broader geotechnical engineering context (Günaydin, 2009; Isik and Ozden, 2013; Shahin and Jaksa, 2006; Kuo et al., 2009; Pooya Nejad et al., 2009), have demonstrated that artificial intelligence (AI) techniques, such as artificial neural networks (ANNs), show great promise in this regard.

In a recent and separate study by the authors, ANNs have been applied to predict the effectiveness of RDC using cone penetration test (CPT) data in relation to the 4-sided impact roller. The model, based on a multi-layer perceptron (MLP), incorporates 4 input parameters, the depth of measurement ( $D$ ), the CPT cone tip resistance ( $q_{ci}$ ) and sleeve friction ( $f_{si}$ ) prior to compaction, and the number of roller passes ( $P$ ). The model predicts a single output variable, i.e. the cone tip resistance ( $q_{cf}$ ) at depth  $D$  after the application of  $P$  roller passes. The ANN model architecture, hence, consists of 4 input nodes, a single output node, and the optimal model incorporates a single hidden layer with 4 hidden nodes. The authors also translated the ANN model into a tractable equation, which was shown to yield reliable predictions with respect to the validation dataset.

This paper aims to develop an accurate tool for predicting the performance of RDC in a range of ground conditions. Specifically, the tool is based on ANNs using DCP test data (ASTM D6951-03, 2003) obtained from a range of projects associated with the Broons BH-1300, 8-tonne, 4-sided impact roller, as shown in Fig. 1. Whilst the DCP is a less reliable test than the CPT, it is nevertheless used widely in geotechnical engineering practice and a model which provides reliable predictions of RDC performance based on DCP data is likely to be extremely valuable to industry.

## 2. ANN model development

In recent years, ANNs have been extensively used in modeling a wide range of engineering problems associated with nonlinearity

and have demonstrated extremely reliable predictive capability. Unlike statistical modeling, ANN is a data-driven approach and hence does not require prior knowledge of the underlying relationships of the variables (Shahin et al., 2002). Moreover, these nonlinear parametric models are capable of approximating any continuous input–output relationship (Onoda, 1995). A comprehensive description of ANN theory, structure and operation is beyond the scope of the paper, but is readily available in the literature (Hecht-Nielsen, 1989; Fausett, 1994; Ripley, 1994; Shahin, 2016).

In this study, the ANN models for predicting the effectiveness of RDC are developed using the PC-based software NEUFRAME version 4.0 (Neuscience, 2000). As mentioned above, the data used for ANN model calibration and validation incorporate DCP test results obtained from several ground improvement projects using the Broons BH-1300, 4-sided impact roller, which has a static mass of 8 tonnes. The data used in this study are summarized in Table 1. It is important to note that the DCP data are obtained at effectively the same location prior to RDC (i.e. 0 pass) and after several passes of the module (e.g. 10, 20 passes), since it is essential to include both pre- and post-compaction conditions in the ANN model simulations. In total, the database contains 2048 DCP records from 12 projects.

ANN model development is carried out using the process outlined by Maier et al. (2010), including determination of appropriate model inputs/outputs, data division, selection of model architecture, model optimization, validation and measures of performance. This methodology is briefly discussed and contextualized below.

### 2.1. Selection of appropriate model inputs and outputs

The most common approach for the selection of data inputs in geotechnical engineering is based on the prior knowledge of the system in question and this is also adopted in the present study. Therefore, the input/output variables of the ANN models are chosen in such a manner that they address the main factors that influence RDC behavior. It is identified that the degree of soil compaction depends upon a number of key parameters, including: the geotechnical properties at the time of compaction, such as ground density, moisture content, and soil type; and the amount of energy imparted to the ground during compaction.

As mentioned previously, in this study, the ANN model is based on DCP test results collected from a range of ground improvement projects involving the 4-sided impact roller. The DCP (ASTM D6951-

Table 1  
Summary of the database of DCP records.

No.	Project	No. of DCP soundings	Soil type		No. of roller passes
			Primary	Secondary	
1	Arndell Park	23	Clay	Silt	0, 5, 10, 20, 25, 30
2	Banyo	2	Clay	Silt	4, 8, 16
3	Banksmeadow	10	Sand	None	0, 10, 20
4	Ferguson	7	Clay	Silt	5, 10, 15
5	Kununurra	5	Sand	None	0, 5, 10, 20, 25, 30, 40, 50, 60
6	Monarto	6	Sand	Gravel	0, 5, 10, 30
7	Outer Harbor	9	Clay	Silt	0, 6, 12, 18, 24
			Sand	Gravel	
8	Pelican Point	8	Clay	Silt	0, 6, 12, 18
9	Penrith	39	Sand	Clay	0, 2, 4, 6, 10, 20
10	Potts Hill	4	Clay	Silt	0, 10, 20, 30, 40
11	Revesby	4	Clay	Silt	0, 5, 10, 15
			Sand	Clay	
			Sand	None	
12	Whyalla	12	Sand	Gravel	0, 8, 16

03, 2003) is one of the most commonly used in situ test methods available, which provides an indication of soil strength in terms of rate of penetration (blows/mm). In this study, the average DCP blow count per 300 mm is used as a measure of the average density improvement with depth as a result of RDC.

Moisture content is not routinely measured in ground improvement projects in practice. Nevertheless, moisture content is considered to be implicitly included in the DCP data, as the number of blows per 300 mm is affected by moisture content. In addition, whilst the natural ground is often characterized as part of site investigations associated with earthworks projects, soil characterization during the process of filling and compacting is not. However, in order to include the soil type in the ANN model, a generalized soil type is defined at each DCP location by adopting primary (dominant) and secondary soil types. The ground improvement projects included in the database can each be characterized into one of 4 distinct soil types: (1) sand–clay, (2) clay–silt, (3) sand–none and (4) sand–gravel. As NEUFRAME requires the allocation of one input node for every parameter, therefore, in this model, the soil type variable represents 4 input nodes.

Hence, in summary, the ANN prediction models developed in this study each have a total of 5 input variables consisting of 8 nodes, together representing: (1) soil type: (a) sand–clay, (b) clay–silt, (c) sand–none, and (d) sand–gravel; (2) average depth below the ground surface,  $D$  (m); (3) initial number of roller passes; (4) initial DCP count (blows/300 mm); and (5) final number of roller passes. The single output variable is the final DCP count (blows/300 mm) at depth  $D$  after compaction.

## 2.2. Data division and pre-processing

In this study, the commonly adopted cross validation technique (Stone, 1974) is used as the stopping criterion, which requires the entire dataset to be divided into 3 subsets: (1) a training set, (2) a testing set, and (3) a validation set. The training set contains 80% of the data (1629 records), whereas the remaining 20% (419 records) is allocated to the validation set. The training set is further subdivided into the training and testing sets in the proportion of 80% (1310 records) and 20% (319 records), respectively. The application of these 3 individual subsets is discussed later.

The distribution of data among the 3 subsets may have a significant impact on model performance (Shahin et al., 2004). Therefore, it is necessary to divide the data into 3 subsets in such a way that they represent the same statistical population exhibiting similar statistical properties (Masters, 1993). The statistical properties considered in this study include the mean, standard deviation, minimum, maximum and range. The present study uses the method of self-organizing maps (SOMs) (Bowden et al., 2002), a detailed explanation of which is given by Kohonen (1982). However, the determination of the optimal map size is an iterative process as there is no absolute rule to select the most favorable map size and thus several map sizes (e.g.  $10 \times 10$ ,  $20 \times 20$ ,  $30 \times 30$ ) are investigated. Once the clusters are generated, samples are randomly selected from each cluster and assigned to each of the 3 data subsets.

Prior to model calibration, data are pre-processed in the form of scaling which ensures that each model variable receives equal attention during model training. Therefore, the output variables are scaled so that they are commensurate with the limits of the sigmoid transfer function that is used in the output layer. Although scaling of the input variables is not necessarily important, as recommended by Masters (1993), in this study, they are also subjected to scaling similar to that for the output variable. In such a way, all the variables are scaled into the selected range of 0.1–0.9 by using Eq.

(1). However, subsequent to model training, the model outputs undergo reverse scaling.

$$I_{\text{scaled}} = a + \frac{(I_{\text{unscaled}} - A)(b - a)}{B - A} \quad (1)$$

where  $A$  and  $B$  are the minimum and maximum values of the unscaled dataset, respectively; and similarly,  $a$  and  $b$  are the minimum and maximum values of the scaled dataset.

## 2.3. Determination of network architecture

The determination of network architecture includes the selection of model geometry and the manner in which information flows through the network. Among many other different types of network architectures, the fully inter-connected, feed-forward type, MLPs are the most common form used in prediction and forecasting applications (Maier and Dandy, 2000). To date, feed-forward networks have been successfully applied to many and varied geotechnical engineering problems (Günaydin, 2009; Kuo et al., 2009; Pooya Nejad et al., 2009).

Network geometry requires the determination of the number of hidden layers and the number of nodes incorporated in each layer. The simplest form of MLP, which is used in this study, consists of 3 layers, including a single hidden layer between the input and output layers. It has been shown that single, hidden layer networks with sufficient connection weights are capable of approximating any continuous function (Cybenko, 1989; Hornik et al., 1989). The ability to use nonlinear activation functions in the hidden and output layers allows the MLP to capture the complexity and nonlinearity of the system in question.

The number of nodes in the input and output layers is restricted by the number of model input and output variables. As mentioned above, this model consists of 8 nodes in the input layer and a single node in the output layer. Selection of the optimal number of hidden layer nodes is again an iterative process. If too few nodes are adopted, the predictive performance of the model is compromised, whereas, if too many nodes are used, the model may be overfitted and thus lack the ability to generalize. The stepwise approach (Shahin et al., 2002) is adopted in this study to obtain the optimal architecture where several ANN models are trained, starting from the simplest form with a single hidden layer node model and successively increasing the number of nodes to 11. According to Caudill (1988), the upper limit of hidden nodes which are needed to map any continuous function for a network with  $I$  input nodes is equal to  $2I + 1$ .

## 2.4. Model optimization

In this study, model optimization, which involves evaluating the optimum weight combination for the ANN, is carried out using the back-propagation algorithm (Rumelhart et al., 1986). It is the most widely used optimization algorithm in feed-forward neural networks and has been successfully implemented in many geotechnical engineering applications (Günaydin, 2009; Pooya Nejad et al., 2009; Shahin and Jaksa, 2006). The back-propagation algorithm is based on the first-order gradient descent rule and has the capability of escaping local minima having appropriately defined the ANNs' internal parameters (Maier and Dandy, 1998). The approach adopted in this study involves the models, consisting of each trial number of hidden nodes, first being trained with the default parameter values (i.e. learning rate = 0.2, momentum term = 0.8) assigned to a random initial weight configuration. The models are then retrained with different combinations of learning rates and momentum terms and the network performance is assessed with respect to the

validation set. However, the networks are vulnerable to being trapped in a local minima if training is initiated from an unfavorable position in the weight space (Shahin et al., 2003a). Therefore, the selected network with optimal parameters is retrained several times and allowed to randomize the initial weight configuration to ensure that model training does not cease at a sub-optimal level.

### 2.5. Stopping criterion

The stopping criterion is used to determine when to cease the ANN model training phase. Since overfitting is a possibility during model training, the cross validation technique is used which, as discussed earlier, requires data division into 3 subsets: training, testing and validation. The training data are used in the model training phase where the connection weights are estimated. The models are considered to achieve the optimal generalization ability when the error measure, with respect to the testing set, is a minimum, having ensured that the training and testing sets are representative of the same statistical population. Although the testing set error shows a reduction at the beginning, it starts to increase when overfitting occurs. Therefore, the optimal network is obtained at the onset of the increase in test data error, assuming that the error surface converges at the global minimum. However, model training is continued for some time, even after the testing error starts to increase initially, to ensure that the model is not trapped in a local minimum (Maier and Dandy, 2000).

### 2.6. Model validation and performance measures

Once the model has been optimized, the network is validated against the independent validation set, which provides a rigorous check of the model's generalization capability. The network is expected to generate nonlinear relationships between the input and output variables rather than simply memorizing the patterns that are contained in the training data (Shahin et al., 2003b). Since the model is assessed with respect to an unseen dataset, the results are significant for the evaluation of network performance.

The measures used in this study in evaluating the networks' predictive performance are the often used root mean squared error (RMSE), mean absolute error (MAE) and coefficient of correlation ( $R$ ). When using the RMSE, larger errors receive much greater attention than smaller errors (Hecht-Nielsen, 1989), whereas MAE provides information on the magnitude of the error. The coefficient of correlation is used to determine the goodness of fit and it describes the relative correlation between the predicted and actual results. The guide proposed by Smith (1993) is used as follows:

- (1)  $|R| \geq 0.8$ : strong correlation exists between two sets of variables;
- (2)  $0.2 < |R| < 0.8$ : correlation exists between two sets of variables; and
- (3)  $|R| \leq 0.2$ : weak correlation exists between two sets of variables.

## 3. Results and discussion

In the following subsections, the results of data division and model optimization are presented followed by the behavior of the optimal network when assessed for robustness using a parametric study.

### 3.1. Results of data division

The SOM size of  $25 \times 25$  is found to be optimal. The statistics of the 3 subsets are presented in Table 2. As expected, in general, the

**Table 2**  
ANN input and output statistics.

Model variable	Dataset	Mean	Standard deviation	Minimum	Maximum	Range
Average depth (m)	Training	0.81	0.51	0.15	1.95	1.8
	Testing	0.82	0.51	0.15	1.95	1.8
	Validation	0.83	0.52	0.15	1.95	1.8
Initial number of roller passes	Training	7.69	10.61	0	50	50
	Testing	7.65	10.44	0	50	50
	Validation	8.71	10.93	0	50	50
Initial DCP count (blows/300 mm)	Training	16.57	10.86	3	65	62
	Testing	15.88	10.64	3	59	56
	Validation	16.31	10.2	3	61	58
Final number of roller passes	Training	21.14	16.25	2	60	58
	Testing	21.16	16.49	2	60	58
	Validation	21.08	16.11	2	60	58
Final DCP count (blows/300 mm)	Training	18.3	11.29	2	84	82
	Testing	17.8	10.81	2	73	71
	Validation	17.93	11.47	3	75	72

statistics are in a good agreement, apart from slight inconsistencies that result from the appearance of singular and rare events in the data, which cannot be replicated in all 3 subsets. It is accepted that ANNs are best used to interpolate within the limits of the data included in the ANN model development process and are best not used for extrapolation.

### 3.2. Results of the optimal ANN model

In selecting the optimal model, several models with a single hidden layer consisting of different numbers of hidden nodes are compared with respect to  $R$ , RMSE and MAE. However, with the parallel aim of parsimony, a model with a smaller number of hidden nodes that performs well, with respect to the validation set and with a consistent performance with the training and testing data, is considered to be optimal. From this perspective, it is observed that the model with 4 hidden nodes yields the best performance with respect to the single hidden layer ANNs.

With the intention of improving prediction accuracy, networks are examined with an additional hidden layer. Similar to the single hidden layer model optimization, several models with different numbers of nodes in the 2 hidden layers are trained and validated. Consequently, the model with 4 and 6 hidden nodes in the first and second hidden layers, respectively, is deemed to be optimal among the 2 hidden layer ANNs. The performance statistics of the selected optimal networks for single and two hidden layer networks are summarized in Table 3.

The optimal single hidden layer model is compared with the optimal two hidden layer model, in terms of model accuracy and model parsimony. It is evident that the prediction accuracy of the two hidden layer model is only marginally better than that of the network with a single hidden layer, given the error difference with respect to the validation set:  $RMSE = 0.73$ ,  $MAE = 0.74$ , and with the difference in correlation:  $R = 0.02$ . Given that the two hidden layer model sacrifices model parsimony for only marginal improvement in performance, it is decided to proceed with the single hidden layer model. This is advantageous, as will be discussed later, as this model facilitates the development of a simple numerical equation which expresses the relationship between the model inputs and output.

As produced by the optimal, single hidden layer ANN model, the plot of predicted versus measured DCP counts with respect to the data in the testing and validation sets is shown in Fig. 2, where the solid line indicates equality. According to the guide proposed by Smith (1993), it can be concluded that there exists very good correlation between the model predictions and the measured values of the final DCP count. However, it is expected that the random errors

**Table 3**  
Performance statistics of the optimal networks with single and two hidden layers.

Model	Dataset	RMSE (blows/300 mm)	MAE (blows/300 mm)	R
Single hidden layer model	Training	6.45	4.88	0.85
	Testing	6.52	4.74	0.83
	Validation	7.54	5.59	0.79
Two hidden layer model	Training	5.72	3.97	0.86
	Testing	5.67	3.88	0.85
	Validation	6.81	4.85	0.81

associated with the input data, as a result of testing uncertainties (operator, procedure, equipment (Orchant et al., 1988)), have adversely affected model performance.

3.3. Robustness of the optimal ANN model

It is essential to conduct a parametric study in order to further confirm the validity, accuracy and generalization ability of the optimal model. It is crucial that the model behavior conforms to the known underlying physical behavior of the system. Therefore, the network’s generalization ability is investigated with respect to a set of synthetic input data generated within the limits of the training dataset. Each input variable is varied in succession, with all other input variables remaining constant at a pre-specified value.

The post-compaction condition of the ground, represented by the final DCP count, is predicted from the optimal ANN model for a given initial DCP count (i.e. 5, 10, 15, and 20 blows/300 mm) in each of the different soil types (i.e. sand–clay, clay–silt, sand–none and sand–gravel) for several, different numbers of roller passes (i.e. 5, 10, 15, 20, 30, and 40 passes). The resulting model predictions are presented in Fig. 3.

It is evident that the final DCP count increases with increasing numbers of roller passes, for a given initial DCP in each soil type, which confirms that the ground is significantly improved with RDC. As such, the graphs verify that the optimal ANN model predictions agree well with the expected behavior based on the impact of RDC. In addition, there are no irregularities in behavior, with respect to each of these variables. As a result, it is concluded that the optimal ANN model is robust when predicting the effectiveness of RDC and can be used with confidence.

Furthermore, the final DCP count is analyzed over average depths between 0.45 m and 1.95 m for each soil type as a function of the number of roller passes, and the results are summarized in

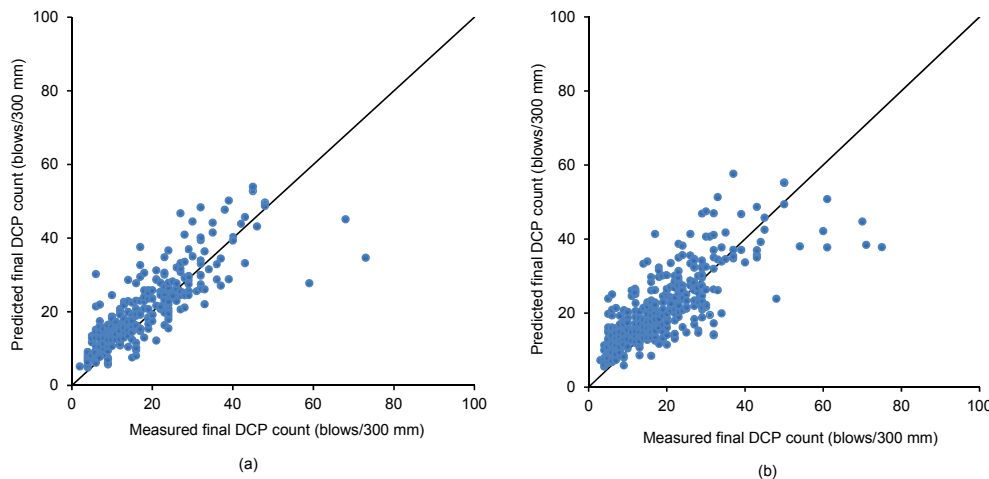


Fig. 2. Measured versus predicted final DCP counts (blows/300 mm) for the optimal ANN model with respect to the (a) testing set and (b) validation set.

Fig. 4. It is noted that the upper 300 mm soil layer is disturbed by the action of RDC module and therefore, for this analysis, model predictions at the average depth of 0.15 m are neglected. However, in all cases, it can be seen that the final DCP count increases as the number of roller passes grows. It can be further observed that the coarse-grained soils undergo greater compaction when fine particles are present in the material. For example, in Fig. 4, it is evident that, for a given initial DCP count, the final DCP count reaches higher values as the number of roller passes increases in the sand–none and sand–clay soils as compared with sand–gravel. In addition, the final DCP count curves exhibit a higher gradient with respect to sand–none and sand–clay soils than that to the sand–gravel. This suggests that, when sand is mixed with some fine particles, the compaction characteristics are improved when compared with sand mixed with gravel. This is consistent with conventional wisdom that some fine particles added to coarse-grained materials enhance the soil’s compaction characteristics. In contrast, it can be seen that the fine-grained soils are more difficult to compact when compared with coarse-grained materials, as indicated by the relatively lower values of final DCP count for the clay–silt soil when compared with the sand–none and sand–clay materials. Again, this is consistent with conventional wisdom.

3.4. MLP-based numerical equation

In order to facilitate the dissemination and deployment of the optimal MLP model, a relatively simple equation is developed to predict the level of ground improvement derived from RDC. The optimal model structure is shown in Fig. 5 and the associated weights and biases are presented in Table 4.

The numerical equation, which relates the input and output variables, can be written as

$$O_{k=13} = f_{sig} \left\{ \theta_k + \sum_{j=9}^{12} \left\{ W_{kj} f_{sig} \left[ \theta_j + \sum_{i=1}^8 (W_{ji} I_i) \right] \right\} \right\} \quad (2)$$

where  $O_k$  is the single output variable, i.e. the final DCP count (blows/300 mm) at average depth  $D$  below the ground;  $\theta_k$  is the threshold value at the output layer and  $W_{kj}$  is the connection weight between the  $j$ th node in the hidden layer and the  $k$ th node in output layer;  $\theta_j$  is the threshold value of the  $j$ th hidden node and  $W_{ji}$  is the connection weight between the  $i$ th input node and the  $j$ th hidden node;  $I_i$  is the  $i$ th input variable; and  $f_{sig}$  is the sigmoid transfer function.

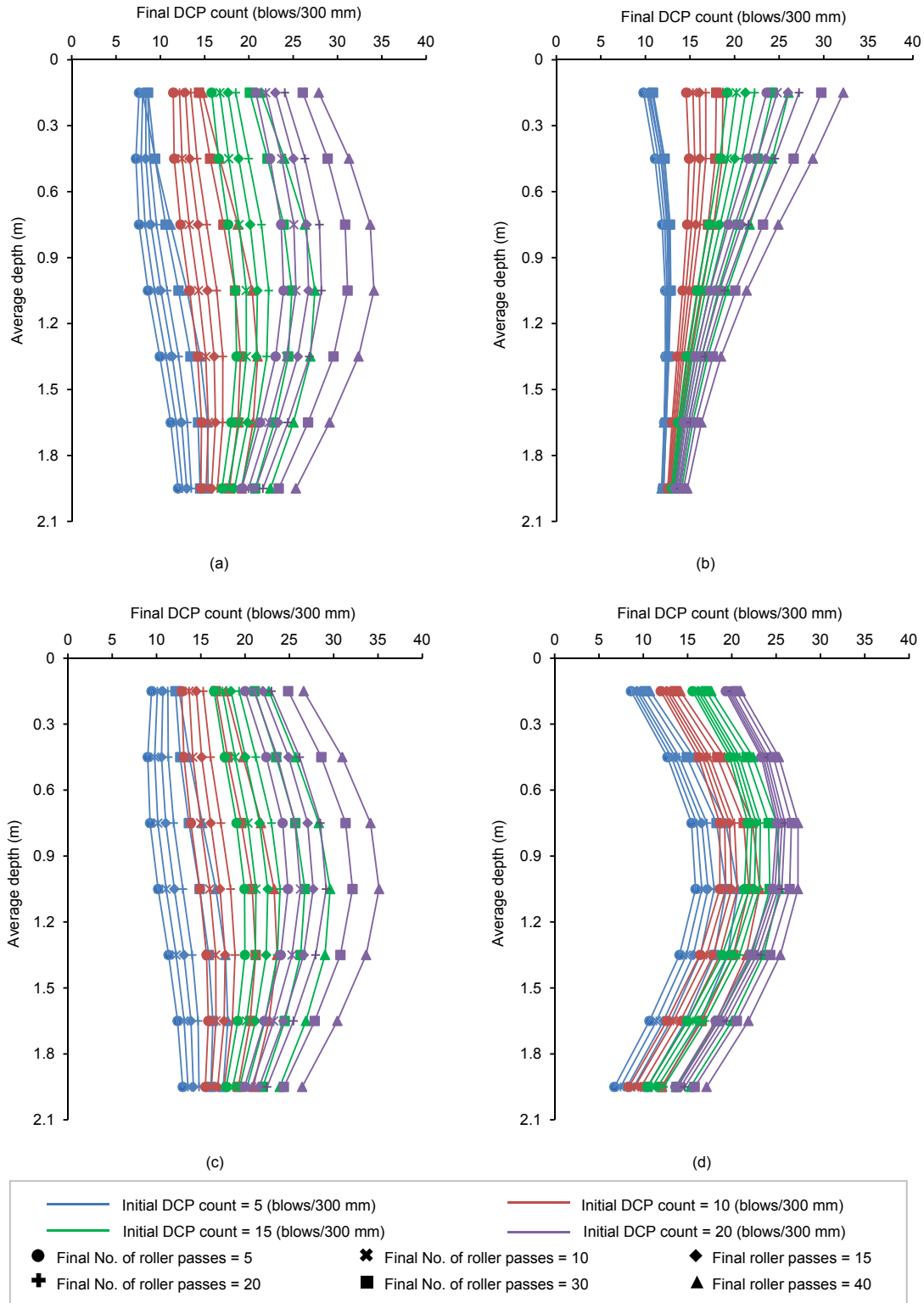


Fig. 3. Variation of final DCP count with respect to initial DCP count and final number of roller passes in (a) sand–clay, (b) clay–silt, (c) sand–none, and (d) sand–gravel.

Eq. (2) can be further simplified as follows:

$$O_{k=13} = \frac{1}{1 + \exp\left\{-\left[\theta_k + \sum_{j=9}^{12} (W_{kj} T_j)\right]\right\}} \quad (3)$$

$$T_{j=9, \dots, 12} = \frac{1}{1 + \exp\left\{-\left[\theta_j + \sum_{i=1}^8 (W_{ji} I_i)\right]\right\}} \quad (4)$$

The variables  $I_1$ ,  $I_2$ ,  $I_3$  and  $I_4$  represent the soil types sand–clay, clay–silt, sand–none and sand–gravel, respectively. These 4 input

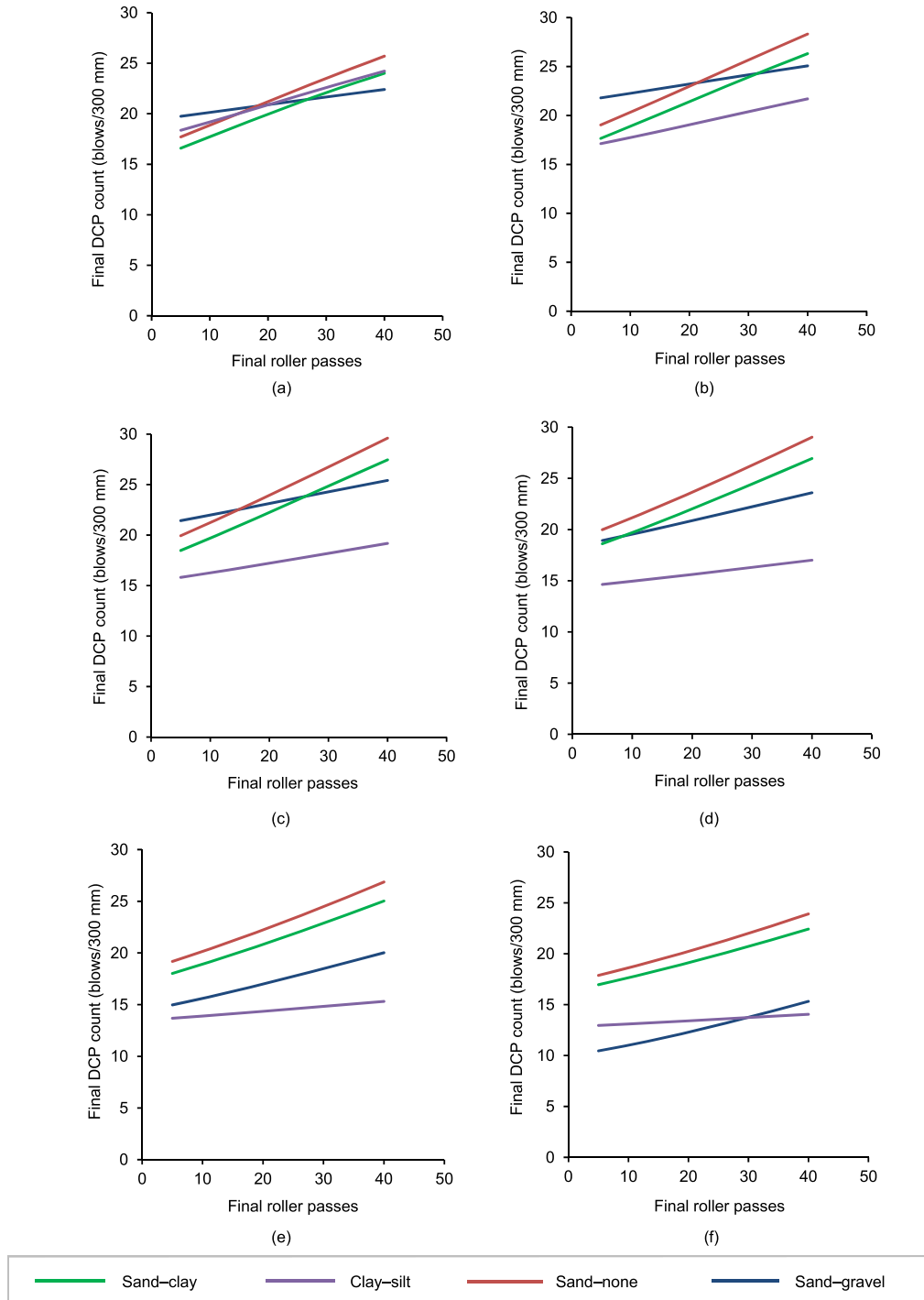


Fig. 4. Variation of final DCP count with final number of roller passes when initial DCP count = 15 and initial passes = 0 in different soil types at depth of (a) 0.45 m, (b) 0.75 m, (c) 1.05 m, (d) 1.35 m, (e) 1.65 m, and (f) 1.95 m.

variables use the binary representation, where the units 1 and 0 are simply used to indicate their presence or absence, respectively. For instance, when the numerical equation (Eq. (2)) is used for the soil type sand–clay, the following is applied:  $I_1 = 1, I_2 = 0, I_3 = 0$  and  $I_4 = 0$ . The remaining input variables, given by  $I_5, I_6, I_7$  and  $I_8$ , represent the average depth,  $D$  (m), the initial of number roller passes, the initial DCP count (blows/300 mm) and the final number of roller passes, respectively.

However, it is noted that the input and output variables are required to be scaled down before using the Eqs. (2)–(4), as mentioned earlier. Therefore, the input variables are scaled between 0.1 and 0.9, by means of Eq. (1), according to the data extremes incorporated in the training set (Table 2), and scaled values are substituted into Eqs. (3) and (4). In addition, the connection weights ( $W_{ji}$  and  $W_{kj}$ ), as well as the threshold levels ( $\theta_j$  and  $\theta_k$ ), are substituted into Eqs. (3) and (4) using the values given in Table 4. As a consequence, the mathematical relationship for the optimal ANN

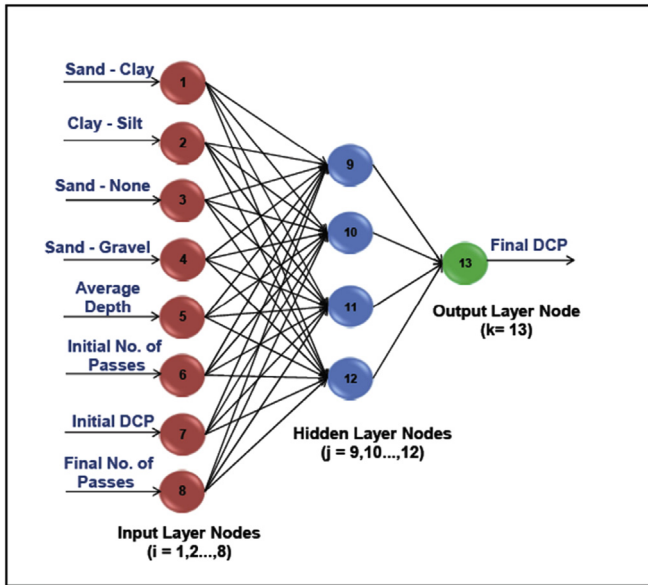


Fig. 5. The structure of the optimal MLP model.

Table 4  
Weights and threshold levels for the optimal ANN model.

Hidden layer node	Weight from node $i$ in input layer to node $j$ in hidden layer ( $W_{ji}$ )								Hidden layer threshold ( $\theta_j$ )
	$i = 1$	$i = 2$	$i = 3$	$i = 4$	$i = 5$	$i = 6$	$i = 7$	$i = 8$	
$j = 9$	-3.128	-5.257	1.216	-0.973	-2.23	-2.481	13.63	0.419	-7.963
$j = 10$	-2.291	-2.225	-3.206	7.35	-2.218	1.76	-12.704	3.431	0.366
$j = 11$	0.082	1.678	-0.014	-1.869	2.932	1.961	-1.286	-0.888	-0.908
$j = 12$	1.486	-0.743	1.482	-0.301	-3.939	-1.45	-4.115	-0.164	1.055
Output layer node	Weight from node $j$ in hidden layer to node $k$ in output layer ( $W_{kj}$ )								Output layer threshold ( $\theta_k$ )
	$j = 9$	$j = 10$	$j = 11$	$j = 12$					
$k = 13$	-2.113	-2.307	-3.725	-3.163					2.269

model incorporating 4 hidden nodes is simplified as follows:

initial random weight configurations. The average of the relative importance is adopted to rank the input variables and the results are summarized in Table 5. As one would expect, the input variables

$$DCP_{final} = \frac{102.5}{1 + \exp(2.113 T_9 + 2.307 T_{10} + 3.725 T_{11} + 3.163 T_{12} - 2.269)} - 8.25 \tag{5}$$

where

$$T_9 = [1 + \exp(3.128I_1 + 5.257I_2 - 1.216I_3 + 0.973I_4 + 0.99I_5 + 0.04I_6 - 0.177I_7 - 0.006I_8 + 7.424)]^{-1}$$

$$T_{10} = [1 + \exp(2.291I_1 + 2.225I_2 + 3.206I_3 - 7.35I_4 + 0.985I_5 - 0.028I_6 + 0.165I_7 - 0.048I_8 + 0.059)]^{-1}$$

$$T_{11} = [1 + \exp(-0.082I_1 - 1.678I_2 + 0.014I_3 + 1.869I_4 - 1.302I_5 - 0.031I_6 + 0.017I_7 + 0.012I_8 + 0.757)]^{-1}$$

$$T_{12} = [1 + \exp(-1.486I_1 + 0.743I_2 - 1.482I_3 + 0.301I_4 + 1.749I_5 + 0.023I_6 + 0.053I_7 + 0.002I_8 - 0.517)]^{-1}$$

Table 5  
Sensitivity analysis of the relative importance of ANN input variables.

Input variable	Relative importance (%)				Average	Rank
	Trial 1	Trial 2	Trial 3	Trial 4		
Soil type	35.55	47.38	35.4	31.9	37.56	1
Average depth, $D$	17.52	11.81	18.73	17.86	16.48	3
Initial No. of roller passes	10.59	9.71	9.89	11.33	10.38	4
Initial DCP count	31.16	24.09	31.13	25.96	28.09	2
Final No. of roller passes	5.17	7.01	4.85	12.94	7.49	5

3.5. Sensitivity analysis: selection of important input parameters

The relative importance of the factors that are significant to ground improvement predictions is identified by carrying out a sensitivity analysis of the selected optimal network. Garson's (1991) algorithm is used in this study, which partitions the network's connection weights to determine the relative importance of each input variable. This method has been used by many researchers (Shahin et al., 2002; Pooya Nejad et al., 2009). The sensitivity analysis is repeated 4 times with the connection weights obtained from the optimal ANN model trained with 4 different



of soil type and initial DCP count are found to be the most important. The relative importance of the input variables appears to be highly sensitive to the initial starting position in the weight space, however, the ranks of the input variables are found to be consistent with each trial.

#### 4. Summary and conclusions

The work presented in this paper investigates the effectiveness of RDC on different soil types and seeks to establish a predictive tool by means of the often applied artificial intelligence technique, i.e. ANNs. The ANN models incorporate a database of ground density data involving DCP test results associated with RDC using the 4-sided, 8-tonne impact roller. ANNs in the form of multi-layer perceptrons are trained with the back-propagation algorithm, where the model input variables are: soil type, average depth,  $D$  (m), initial number of roller passes, initial DCP count (blows/300 mm) and the final number of roller passes, with the sole output being the final DCP count (blows/300 mm) at depth  $D$  after compaction. It is found that the selected optimal model, with a single hidden layer incorporating 4 nodes, is capable of effectively capturing the density development with respect to the number of impact roller passes and the associated subsurface conditions. The resulting optimal ANN model demonstrates very good accuracy, with  $R$  of 0.79,  $RMSE$  of 7.54 and  $MAE$  of 5.59, when validated against a set of unseen data. In addition, a parametric study is carried out to assess the generalization ability and robustness of the optimal model, where the results emphasize that the model's responses agree well with the expected physical relationships among the parameters. Therefore, the model is recommended as a reliable tool to predict ground improvement as a result of RDC.

A sensitivity analysis is also carried out where the relative importance of the parameters affecting ground improvement is investigated. It is identified that the soil type and the initial DCP count (blows/300 mm) are the dominant parameters. Subsequently, based on the optimal model characteristics, a simplified numerical equation that defines the functional form of the relationship between the model inputs and output is formulated to assist with hand calculations in practice.

#### Conflict of interest

We wish to confirm that there are no known conflicts of interest associated with this publication and there has been no significant financial support for this work that could have influenced its outcome.

#### Acknowledgements

This research was supported under Australian Research Council's Discovery Projects funding scheme (project No. DP120101761). The authors wish to acknowledge Mr. Stuart Bowes at Broons Hire (SA) Pty. Ltd. for his kind assistance and continuing support, especially in providing access to the in situ test results upon which the numerical models are based. The authors are also grateful to Mr. Brendan Scott for his contribution to this work.

#### References

ASTM D6951-03. Standard test method for use of the dynamic cone penetrometer in shallow pavement applications. West Conshohocken, USA: ASTM International; 2003.

Avalle DL. Use of the impact roller to reduce agricultural water loss. In: Proceedings of the 9th ANZ Conference on Geomechanics. Auckland: Citeseer; 2004. p. 513–8.

Avalle DL. Reducing haul road maintenance costs and improving tyre wear through the use of impact rollers. In: Proceedings of the Mining for Tyres Conference, Perth, Australia; 2006.

Bowden GJ, Maier HR, Dandy GC. Optimal division of data for neural network models in water resources applications. *Water Resources Research* 2002;38(2):2–11.

Caudill M. Neural networks primer, part III. *AI Expert* 1988;3(6):53–9.

Clegg B, Berrangé AR. The development and testing of an impact roller. *The Civil Engineer in South Africa* 1971;13(3):65–73.

Clifford JM. Impact rolling and construction techniques. In: Australian Road Research Board (ARRB) Conference, Perth, Australia; 1976.

Clifford JM. The impact roller – problem solved. *The Civil Engineer in South Africa* 1978;20(2):321–4.

Cybenko G. Approximation by superpositions of a sigmoidal function. *Mathematics of Control, Signals and Systems* 1989;2(4):303–14.

Fausett LV. Fundamentals of neural networks: architectures, algorithms, and applications. Englewood Cliffs: Prentice-Hall Inc.; 1994.

Garson DG. Interpreting neural network connection weights. *AI Expert* 1991;6(4):47–51.

Günaydin O. Estimation of soil compaction parameters by using statistical analyses and artificial neural networks. *Environmental Geology* 2009;57:203–15.

Hecht-Nielsen R. Theory of the backpropagation neural network. In: International Joint Conference on Neural Networks (IJCNN); 1989. p. 593–605.

Hornik K, Stinchcombe M, White H. Multilayer feedforward networks are universal approximators. *Neural Networks* 1989;2(5):359–66.

Isik F, Ozden G. Estimating compaction parameters of fine- and coarse-grained soils by means of artificial neural networks. *Environmental Earth Sciences* 2013;69(7):2287–97.

Jaksa MB, Scott BT, Mentha NL, Symons AT, Pointon SM, Wrightson PT, Syamsuddin E. Quantifying the zone of influence of the impact roller. In: Proceedings of ISSMGE-TC 211 International Symposium on Ground Improvement, Brussels; 2012.

Kohonen T. Self-organized formation of topologically correct feature maps. *Biological Cybernetics* 1982;43(1):59–69.

Kuo YL, Jaksa MB, Lyamin AV, Kagawa WS. ANN-based model for predicting the bearing capacity of strip footing on multi-layered cohesive soil. *Computers and Geotechnics* 2009;36(3):503–16.

Maier HR, Dandy GC. The effect of internal parameters and geometry on the performance of back-propagation neural networks: an empirical study. *Environmental Modelling and Software* 1998;13(2):193–209.

Maier HR, Dandy GC. Neural networks for the prediction and forecasting of water resources variables: a review of modelling issues and applications. *Environmental Modelling and Software* 2000;15(1):101–24.

Maier HR, Jain A, Dandy GC, Sudheer KP. Methods used for the development of neural networks for the prediction of water resource variables in river systems: current status and future directions. *Environmental Modelling and Software* 2010;25(8):891–909.

Masters T. Practical neural network recipes in C++. San Diego, California, USA: Academic Press; 1993.

Neurosciences. Neuframe version 4.0. Southampton, Hampshire, UK: Neurosciences Corporation; 2000.

Onoda T. Neural network information criterion for the optimal number of hidden units. In: Proceedings of the International Conference on Neural Networks. Perth, Western Australia: IEEE; 1995. p. 275–80.

Orchant CJ, Kulhawy FH, Trautmann CH. Critical evaluation of in-situ test methods and their variability. Report EL-5507, vol. 2. Palo Alto: Electric Power Research Institute; 1988.

Pinard MI. Innovative developments in compaction technology using high energy impact compactors. In: Proceedings of the 8th Australia New Zealand Conference on Geomechanics. Consolidating Knowledge. Australian Geomechanics Society; 1999. p. 775–81.

Pooya Nejad F, Jaksa MB, Kakhi M, McCabe BA. Prediction of pile settlement using artificial neural networks based on standard penetration test data. *Computers and Geotechnics* 2009;36:1125–33.

Ripley BD. Neural networks and related methods for classification. *Journal of the Royal Statistical Society: Series B (Methodological)* 1994;56(3):409–56.

Rumelhart DE, Hinton GE, Williams RJ. Learning representations by back-propagating errors. *Nature* 1986;323:533–6.

Shahin MA. State-of-the-art review of some artificial intelligence applications in pile foundations. *Geoscience Frontiers* 2016;7(1):33–44.

Shahin MA, Jaksa MB. Pullout capacity of small ground anchors by direct cone penetration test methods and neural networks. *Canadian Geotechnical Journal* 2006;43(6):626–37.

Shahin MA, Maier HR, Jaksa MB. Predicting settlement of shallow foundations using neural networks. *Journal of Geotechnical and Geoenvironmental Engineering* 2002;128(9):785–93.

Shahin MA, Maier HR, Jaksa MB. Settlement prediction of shallow foundations on granular soils using B-spline neurofuzzy models. *Computers and Geotechnics* 2003a;30(8):637–47.

Shahin MA, Maier HR, Jaksa MB. Closure to "Predicting settlement of shallow foundations using neural networks" by Mohamed A. Shahin, Holger R. Maier, and Mark B. Jaksa. *Journal of Geotechnical and Geoenvironmental Engineering* 2003b;129(12):1175–7.

Shahin MA, Maier HR, Jaksa MB. Data division for developing neural networks applied to geotechnical engineering. *Journal of Computing in Civil Engineering* 2004;18(2):105–14.

Smith M. Neural networks for statistical modeling. New York: Nostrand-Reinhold; 1993.

Stone M. Cross-validatory choice and assessment of statistical predictions. *Journal of the Royal Statistical Society: Series B (Methodological)* 1974;36(2):111–47.



**R.A.T.M. Ranasinghe** is currently pursuing a Ph.D. in civil engineering in the School of Civil, Environmental and Mining Engineering at the University of Adelaide, Australia. She completed the bachelor of the science of engineering (Honours) degree in civil engineering with a first class in 2011 from the University of Moratuwa, Sri Lanka. She is currently conducting a research in developing a robust predictive tool to forecast the performance of rolling dynamic compaction using artificial intelligence (AI) techniques. Her research interests include ground improvement, AI techniques, and computer applications in geotechnical engineering. She is a member of the Institution of Engineers Sri Lanka (IESL) and Australian Geomechanics Society (AGS).



**Y.L. Kuo** is currently a research associate in School of Civil, Environmental and Mining Engineering, The University of Adelaide, Australia, after completing his Ph.D. in the same university. He is working in a number of specialized geotechnical areas, including ground improvement, application of artificial intelligence, numerical modeling, site investigation strategy, engineering education, and spatial variability of soil properties.



**M.B. Jaksa** is professor of geotechnical engineering at the University of Adelaide, Australia, where he has been since 1988. He is the current Vice President for Australasia of the International Society for Soil Mechanics and Geotechnical Engineering and a former Chair of the Australian Geomechanics Society. His research interests include artificial intelligence, spatial variability of soils, ground improvement and geo-engineering education.



**F. Pooya Nejad** is a full-time member at the University of Adelaide. Dr. Pooya Nejad has a Ph.D. degree in geotechnical engineering and is an expert in artificial neural networks (ANNs), having developed several ANN models related to geotechnical engineering. He has more than 20 years of university teaching experience in both structural and geotechnical engineering. He has also practiced as a consulting structural and geotechnical engineer in Iran and Australia.